



Supplement of

Distributed surface mass balance of an avalanche-fed glacier

Marin Kneib et al.

Correspondence to: Marin Kneib (marin.kneib@gmail.com)

The copyright of individual parts of the supplement might differ from the article licence.

Table S1: Parameter values used for the SMB inversions. σ_{dh} is the uncertainty in rate of elevation change (standard deviation in a normal distribution centred around 0), σ_v is the uncertainty in surface velocity (standard deviation in a normal distribution centred around 0 for the SIA and F2019 modelling approaches), σ_h is the uncertainty in ice thickness, and σ_s is the uncertainty in surface elevation.

| Parameters for Monte Carlo simulations | SIA | F2019 | IGM |
|---|---|-------|-------------------------|
| $\rho_{\nabla q}$ (kg.m ⁻³) | 900 | | |
| ρ_{dH} (kg.m ⁻³) | Accumulation area: 600 Ablation area: 900 Mixed zone: uniform distribution [600; 900] | | |
| γ (-) | uniform distr. [0.8; 1] | | from inversion |
| σ_{dH} (m.yr ⁻¹) | 0.07 | | |
| σ_v (m.yr ⁻¹) | 2.4 | | uniform distr. [0; 2.4] |
| σ_h (m) | Sequential Gaussian Simulations | | uniform distr. [0; 50] |
| σ_s (m) | NA | | uniform distr. [0; 0.5] |

Table S2: Maximum snow line elevation at the end of the summer on the Rognons tributary and the Argentière main glacier trunk.

| Pléiades acquisition date | Max. SLA Rognons (m a.s.l.) | Max. SLA main glacier trunk (m a.s.l.) |
|---------------------------|-----------------------------|--|
| 19/08/2012 | 3030 | 2960 |
| 30/08/2015 | 3020 | 2970 |
| 14/08/2017 | 2990 | 2980 |
| 08/09/2018 | 3070 | 2960 |
| 25/08/2019 | 3020 | 2970 |
| 17/09/2020 | 2950 | 2940 |
| 15/08/2021 | 2930 | 2820 |
| Mean | 3000 | 2940 |

Table S3: Minimum, mean and maximum value of the glacier-wide mean flux divergence obtained from the 100 distributed thicknesses of the F2019, SIA and IGM modelling approaches. The 2 step filter includes the filtering (using a local gaussian filter, with a scaling length equal to four ice thicknesses) of the velocity and thickness gradients prior to the flux divergence calculation, and then the filtering of the flux divergence. The 1 step filter only includes the filtering of the flux divergence.

| Glacier-wide mean flux divergence (m/yr) | 2 step filter | | 1 step filter | | IGM |
|--|---------------|------|---------------|-------|-------|
| | F2019 | SIA | F2019 | SIA | |
| Minimum | 0.12 | 0.30 | - 0.09 | -0.22 | -0.23 |
| Mean | 0.38 | 0.59 | 0.23 | 0.20 | 0.11 |
| Maximum | 0.56 | 0.95 | 0.45 | 0.73 | 0.19 |

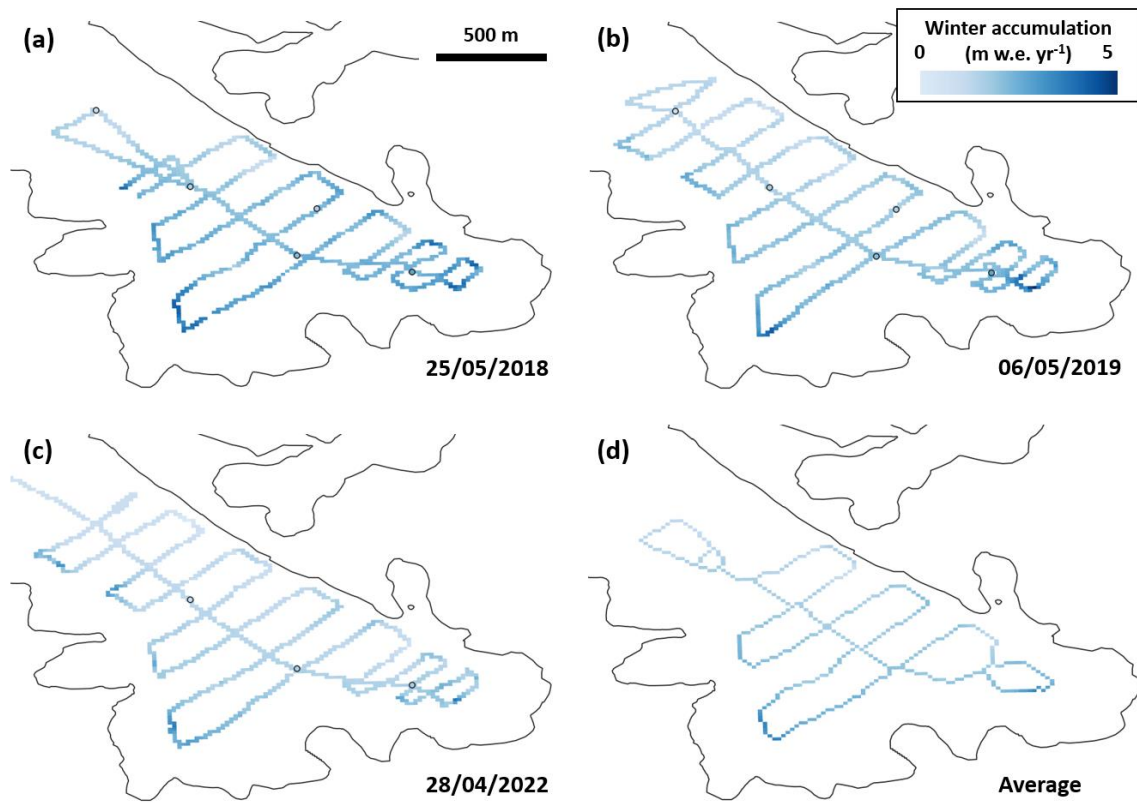


Figure S1: Winter accumulation from GPR surveys. The circled dots correspond to the winter accumulation measurements from GLACIOCLIM.

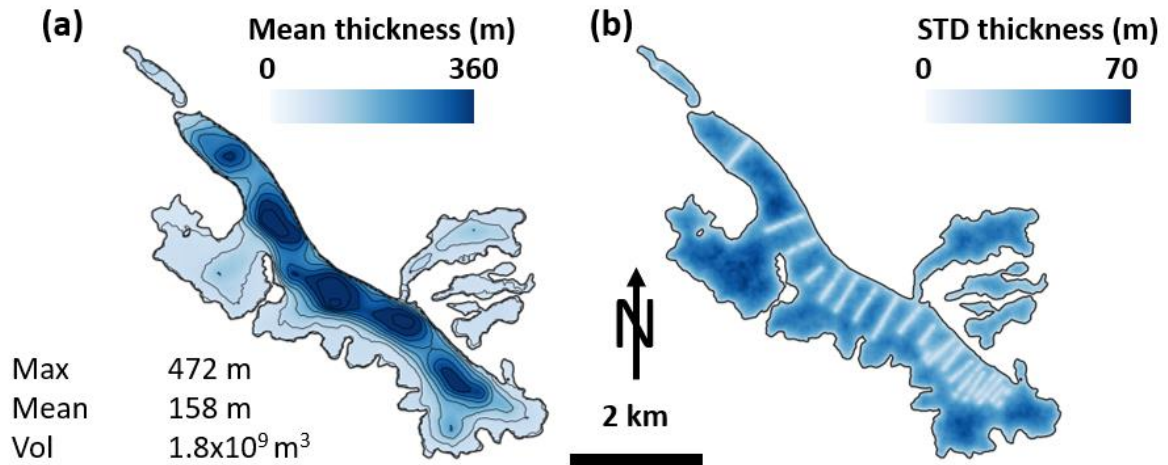


Figure S2: (a) mean and (b) standard deviation of the 100 SGSs applied to the SIA thickness. The black thickness contour lines are spaced every 50 m. The numbers in panel (a) indicate the maximum and mean thickness and the total glacier volume. The black glacier outlines were derived from a Pléiades orthoimage acquired on 08/09/2020.

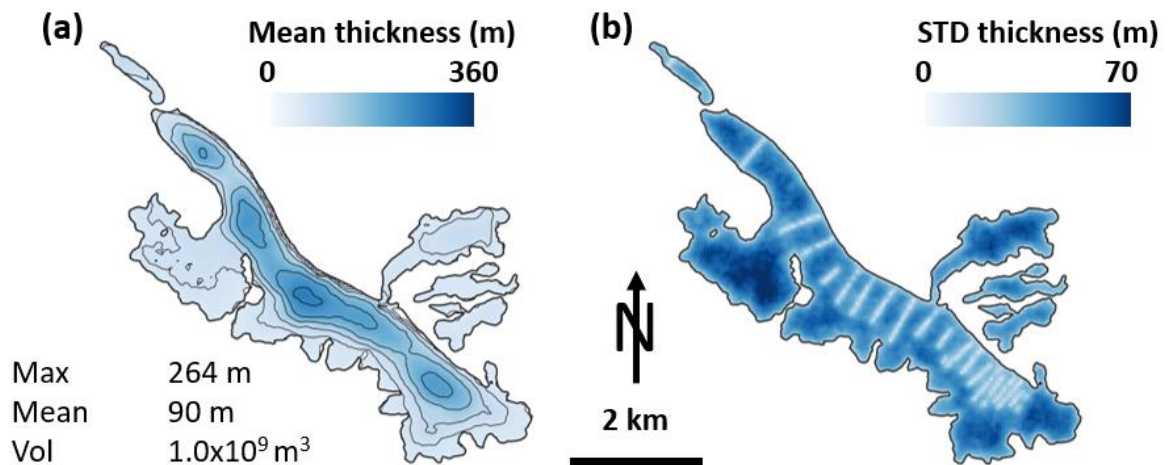


Figure S3: (a) mean and (b) standard deviation of the 100 SGSs applied to the F2019 thickness. The black thickness contour lines are spaced every 50 m. The numbers in panel (a) indicate the maximum and mean thickness and the total glacier volume. The black glacier outlines were derived from a Pléiades orthoimage acquired on 08/09/2020.

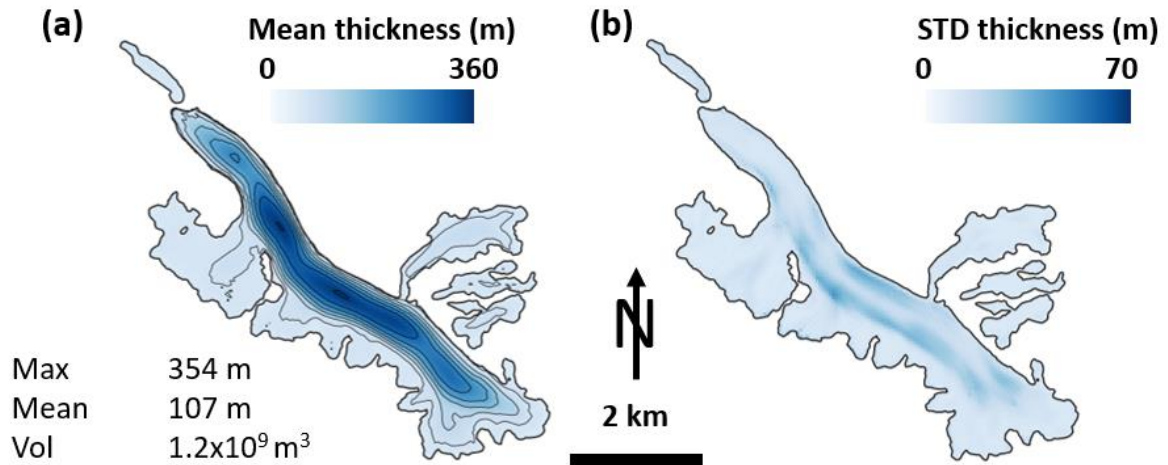


Figure S4: (a) mean and (b) standard deviation of the 100 ice thickness inversions obtained with IGM. The black thickness contour lines are spaced every 50 m. The numbers in panel (a) indicate the maximum and mean thickness and the total glacier volume. The black glacier outlines were derived from a Pléiades orthoimage acquired on 08/09/2020.

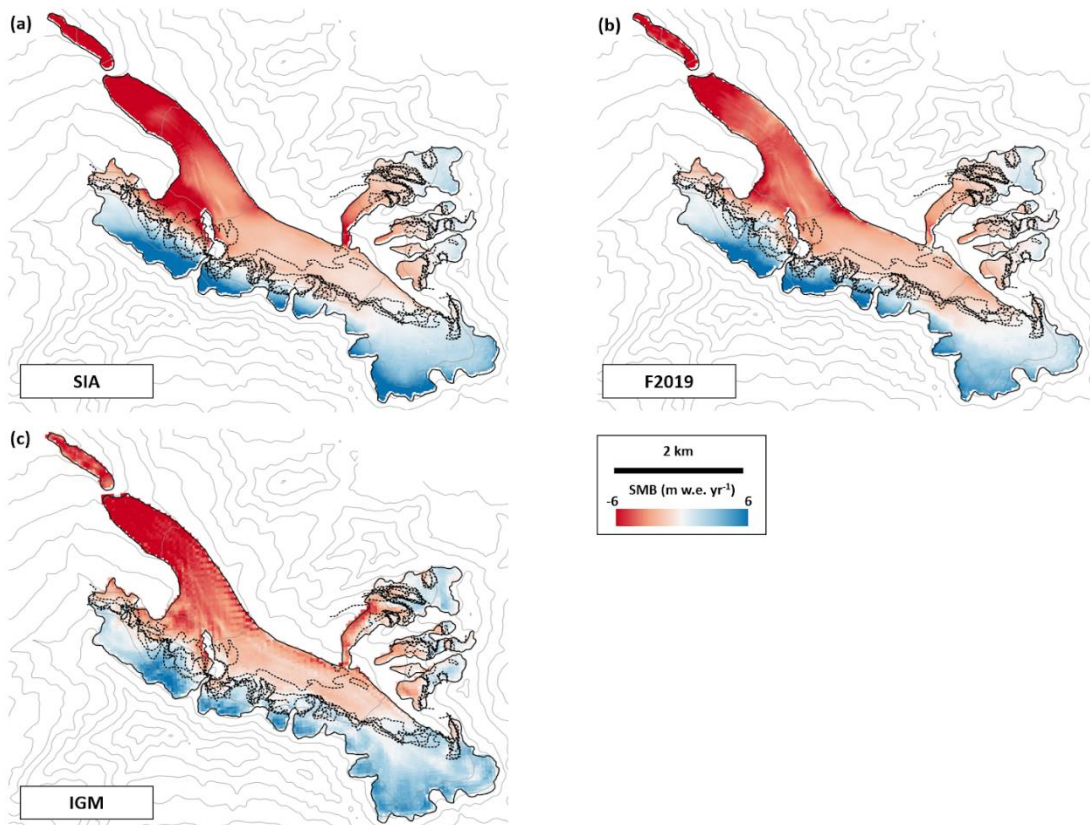


Figure S5: distributed SMB obtained with the different modelling approaches. The dashed black lines indicate the end-of-season snow lines extracted from the Pléiades orthoimages over the 2012-2021 period. The black glacier outlines were derived from a Pléiades orthoimage acquired on 08/09/2020.

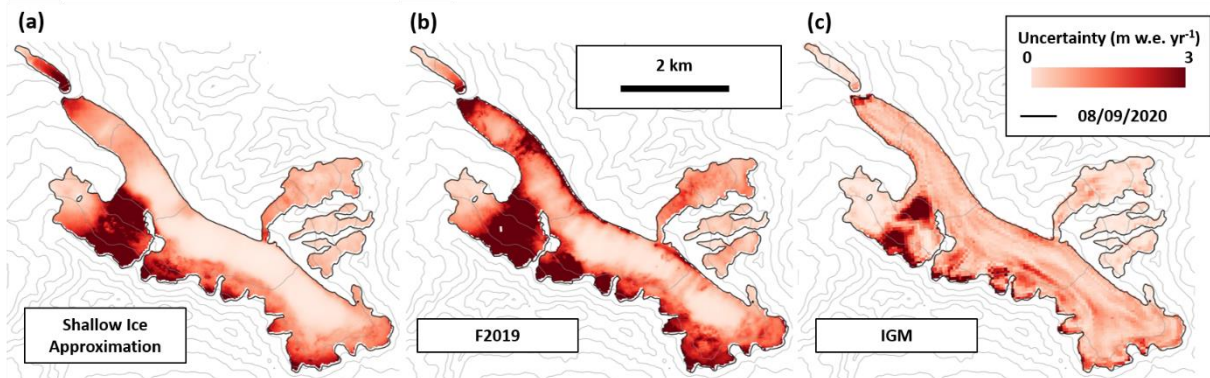


Figure S6: SMB uncertainties with (a) the SIA, (b) the F2019 and (c) the IGM modelling approaches.

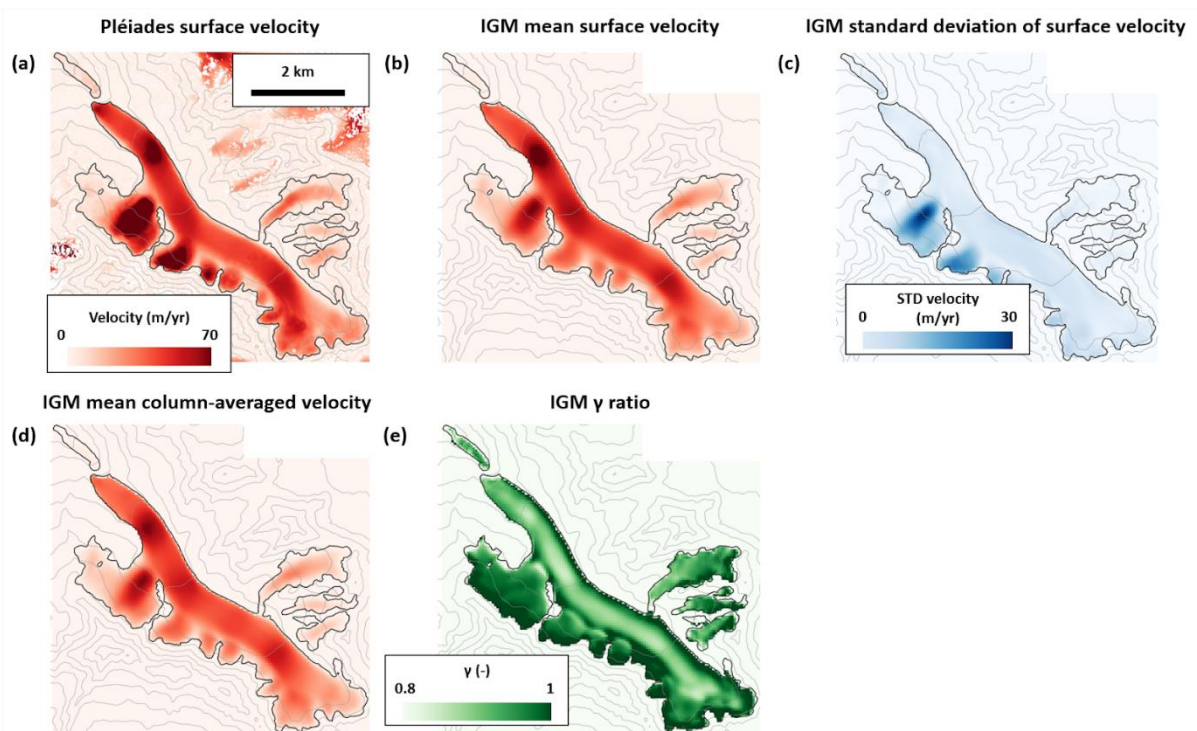


Figure S7: (a) Surface velocity from Pléiades images. (b) Mean surface velocity of the 100 velocity fields obtained with the IGM inversion. (c) Standard deviation of the 100 velocity fields obtained with the IGM inversion. (d) Mean column-averaged velocity of the 100 3D velocity fields obtained with the IGM inversion. (e) Ratio of mean column-averaged velocity and mean surface velocity, corresponding to the γ ratio (Eq. 2). A value of 0.8 corresponds to a shearing-dominated flow and 1 corresponds to sliding-dominated flow. The black glacier outlines were derived from a Pléiades orthoimage acquired on 08/09/2020.

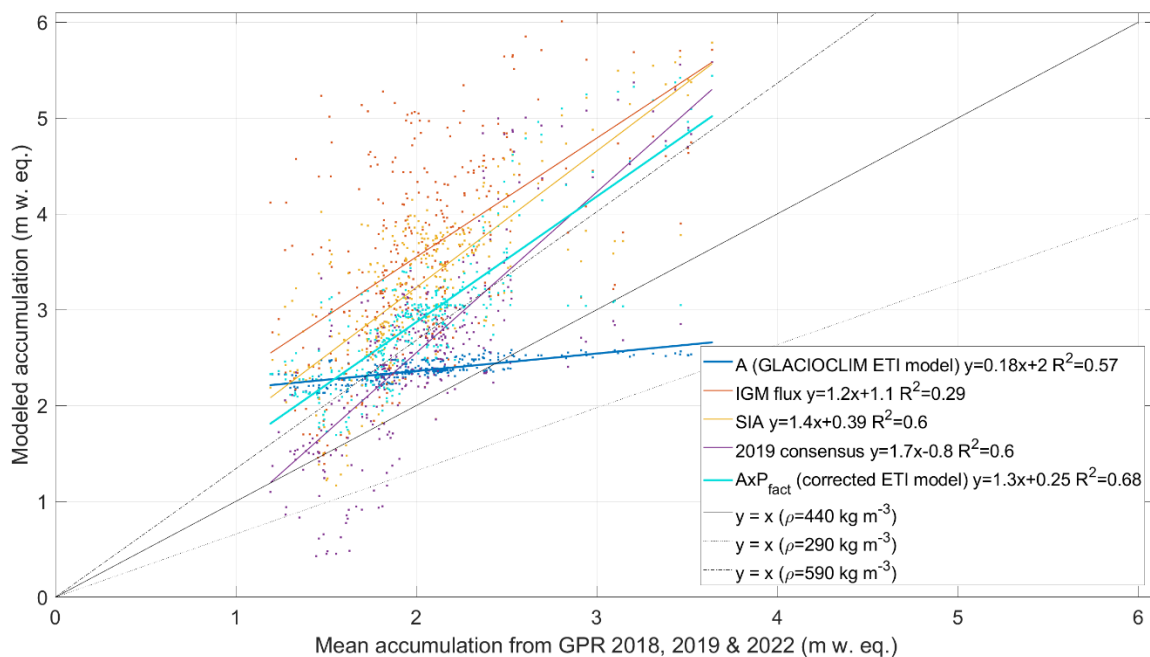


Figure S8: Modelled accumulation from the GLACIOCLIM ETI model (A, in dark blue), the three SMB inversions (in red, yellow and purple) and the corrected ETI model ($A \cdot P_{fact}$, in turquoise) as a function of the mean winter accumulation measured with GPR in the upper accumulation area of Argentière Glacier. The respective equations and R^2 values of the regression lines are indicated in the legend. The black lines correspond to the $y=x$ functions for density values of $440 \pm 150 \text{ kg m}^{-3}$ to convert the snow depths measured with GPR to snow water equivalent.

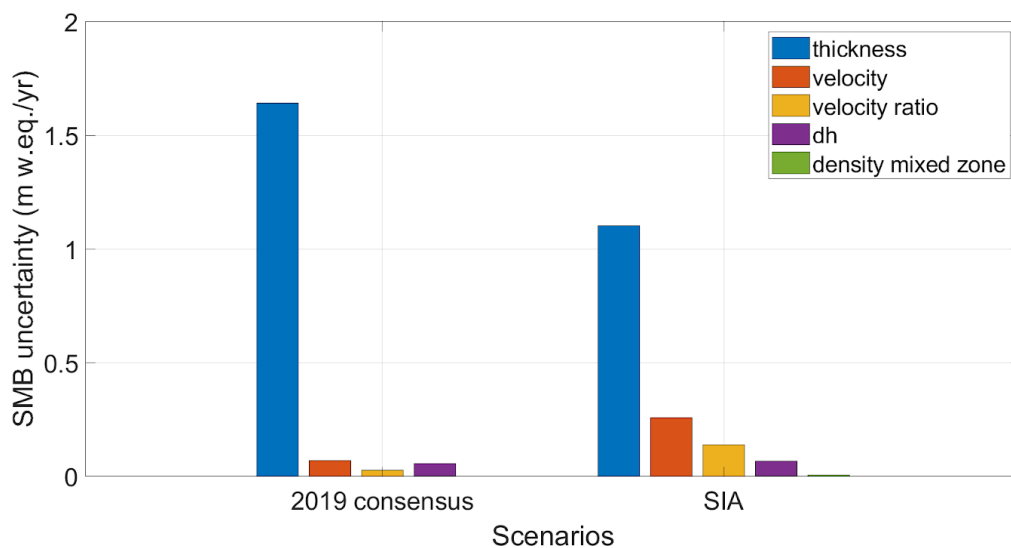


Figure S9: Spatially averaged mean uncertainty for the F2019 and SIA modelling approaches following a one-at-time sensitivity test with 100 simulations for each individual parameter.

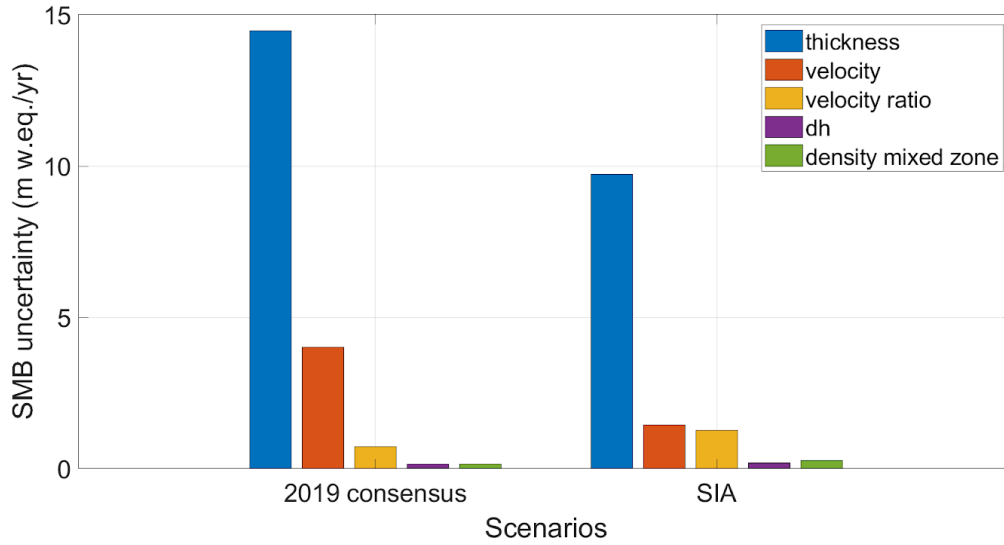


Figure S10: Maximum uncertainty for the F2019 and SIA modelling approaches following a one-at-a-time sensitivity test with 100 simulations for each individual parameter.

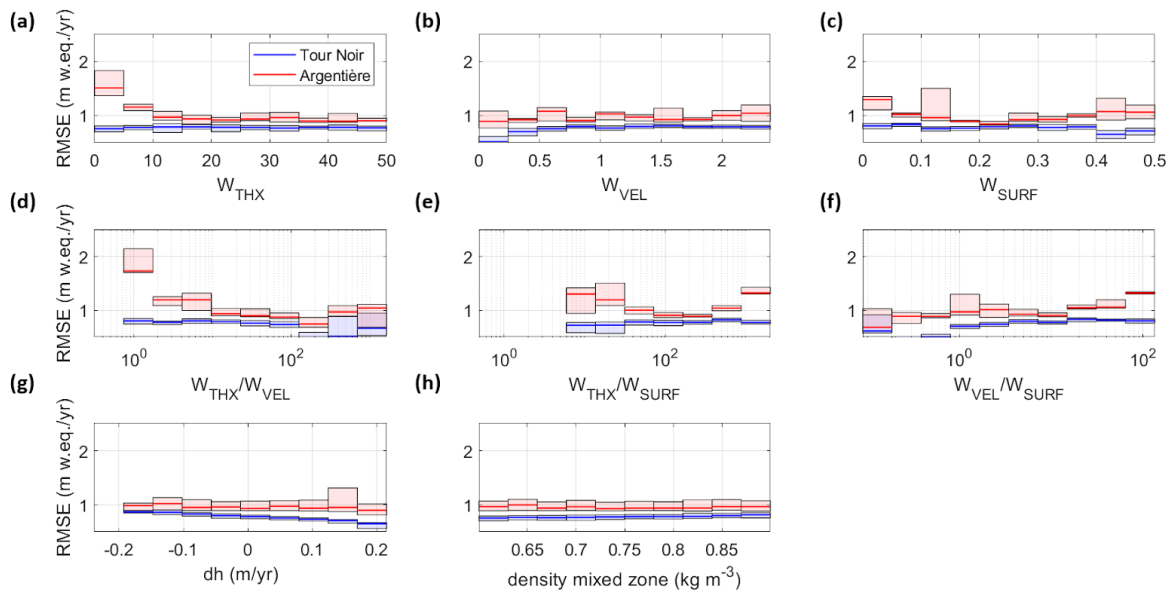


Figure S11: RMSE of SMB at stake locations for the Argentière (red) and Tour Noir (blue) stakes as a function of (a) the prescribed weight of the thickness observations, (b) the prescribed weight of the surface velocity observations, (c) the prescribed weight of the surface (or DEM) observations, (d) the ratio of the thickness and velocity observation weights, (e) the ratio of the thickness and surface observation weights, (f) the ratio of the velocity and surface observation weights, (g) the added elevation change value, (h) the added density value in the mixed zone. These values were obtained from the Monte Carlo simulations of SMB for the IGM inversion. Lower bounds correspond to the 25th percentile and the upper bounds to the 75th percentile. The lines indicate the median value.

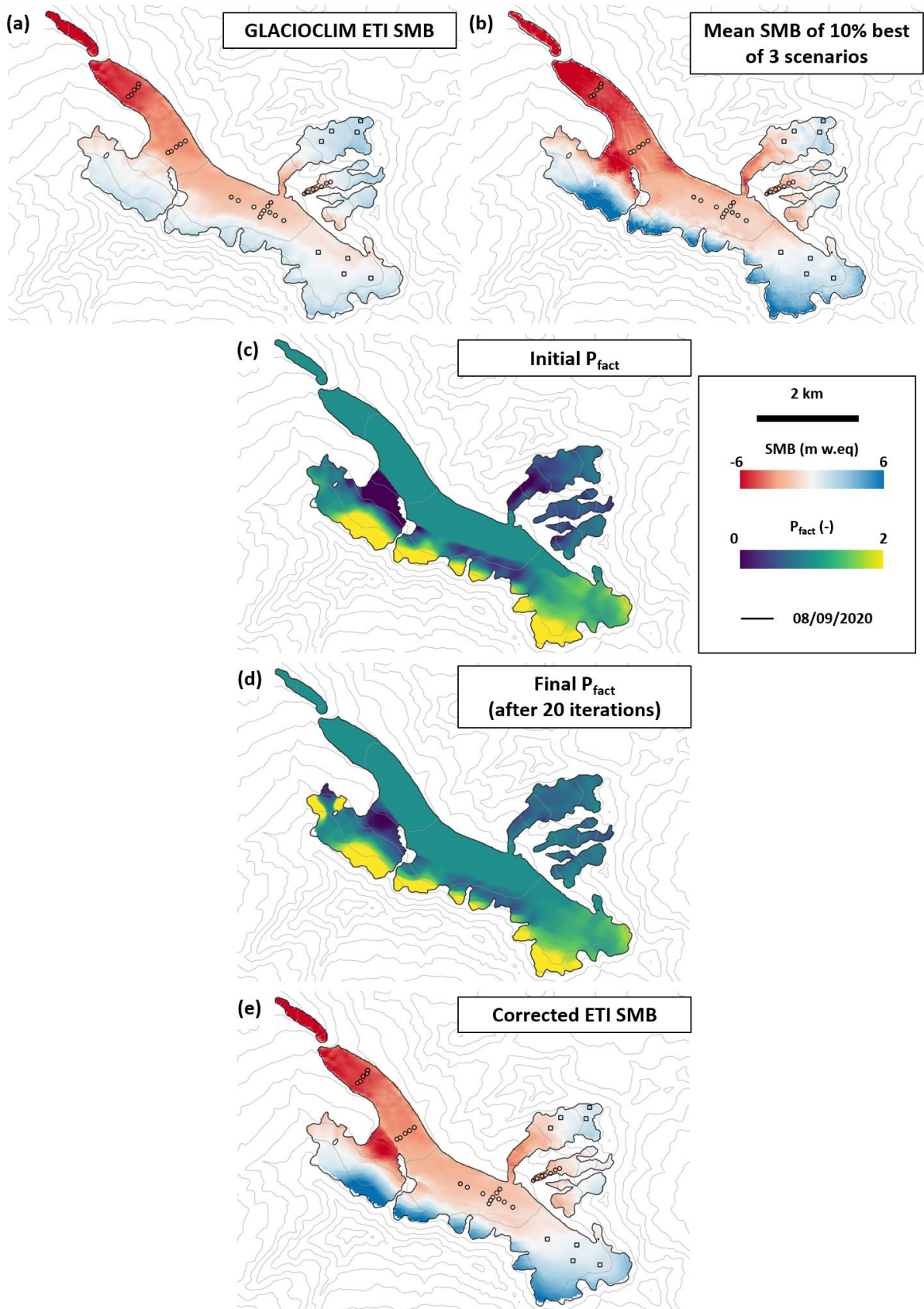


Figure S12: (a) Mean annual SMB over the period 2012-2021, as obtained from the GLACIOCLIM ETI SMB model (section 2.10), with the mean annual 2012-2021 stake measurements at the stake locations

(circles indicate stakes in the ablation zone and squares show stakes in the accumulation zone). (b) Mean SMB of the 10% best inverted SMBs (based on their fit with the in situ measurements) of the three modelling approaches. (c) Precipitation correction factor obtained from the direct comparison of (a) and (b). (d) Precipitation correction factor after 20 iterations (final P_{fact}) of the SMB model. (e) Mean SMB obtained from the corrected ETI model. The grey elevation contour lines are spaced every 200 m.

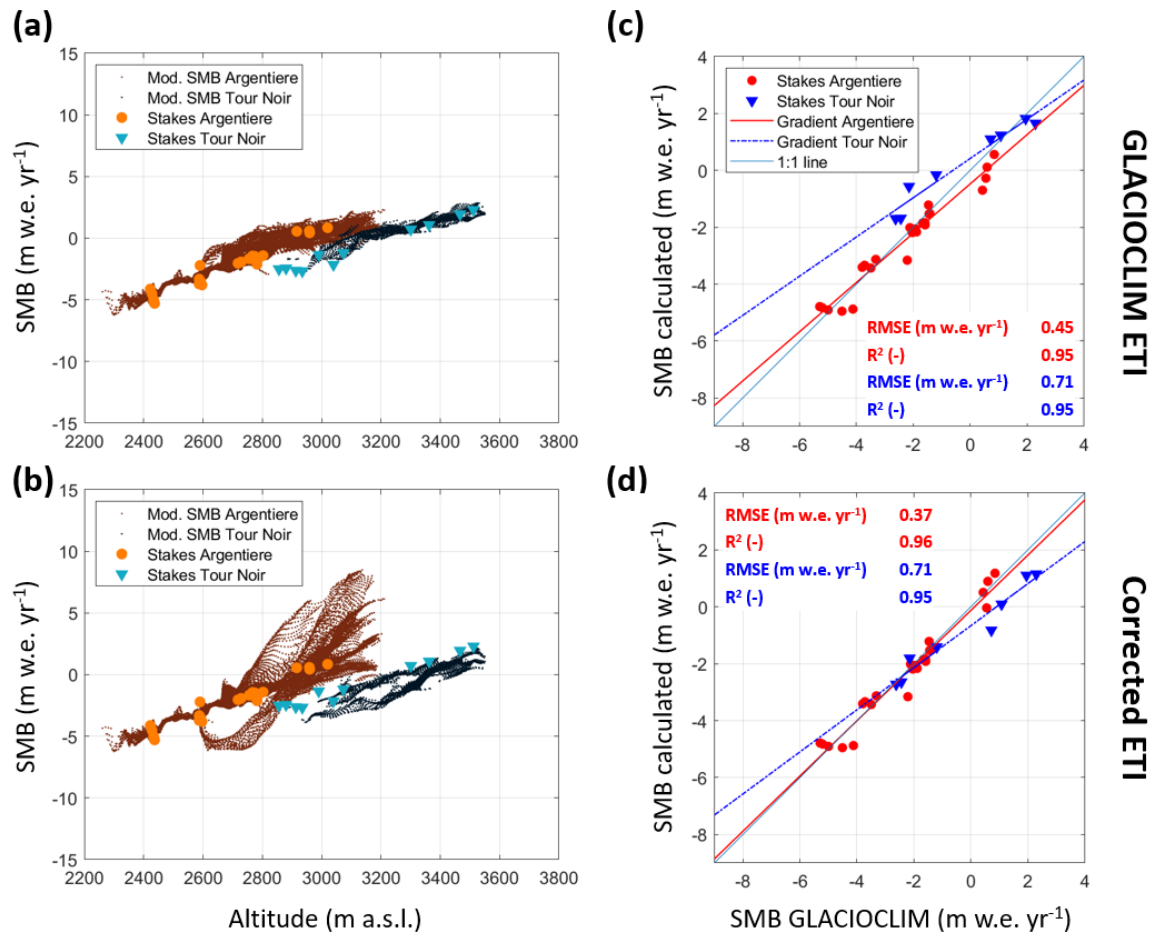


Figure S13: (a-b) Altitudinal patterns of mean annual ETI SMB before and after correction with P_{fact} and of the mean annual mass balances over the period 2012-2021 from the stake measurements. (c-d) Direct comparison of mean annual ETI SMB before and after correction with P_{fact} , with the mean annual mass balances over the period 2012-2021 from the stake measurements, at the stake locations.

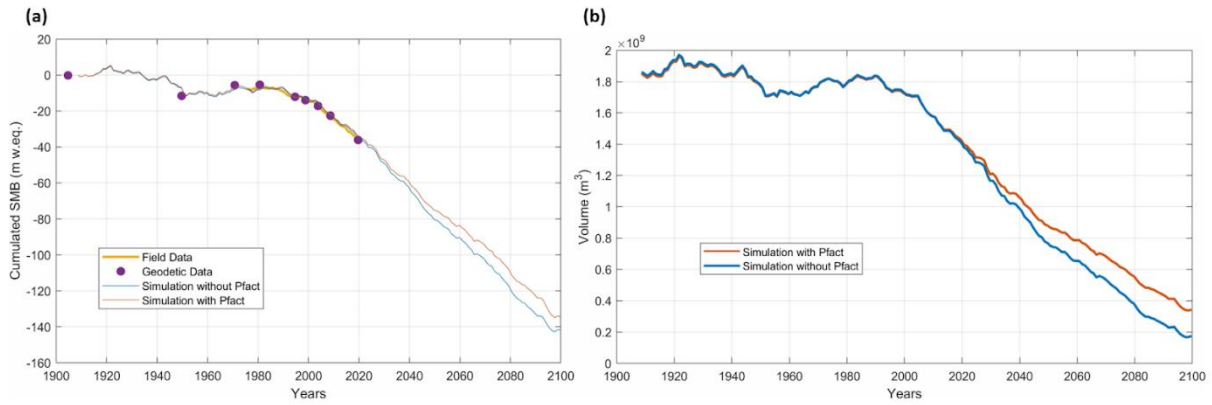


Figure S14: (a) Cumulative surface mass balance and (b) total volume (including Tour Noir) for the period 1907-2100 using the CMIP 5 RCP 4.5 climate scenario for the GLACIOCLIM (simulation without P_{fact}) and corrected (simulation with P_{fact}) scenarios.

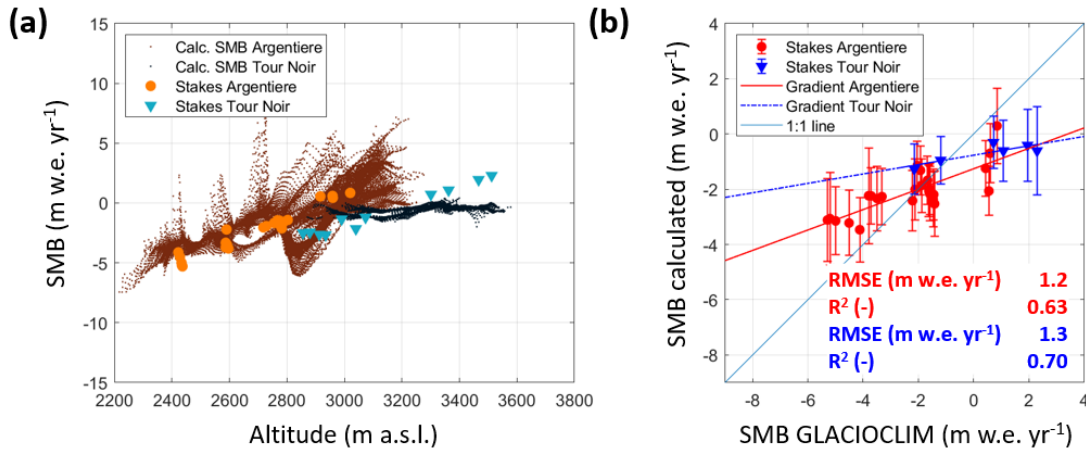


Figure S15: (a) Altitudinal patterns of mean annual SMB calculated with the F2019 thickness and the velocity data from Millan et al. (2022), and of the mean annual mass balances over the period 2012-2021 from the stake measurements. (b) Direct comparison of mean annual calculated SMB, with the mean annual mass balances over the period 2012-2021 from the stake measurements, at the stake locations.

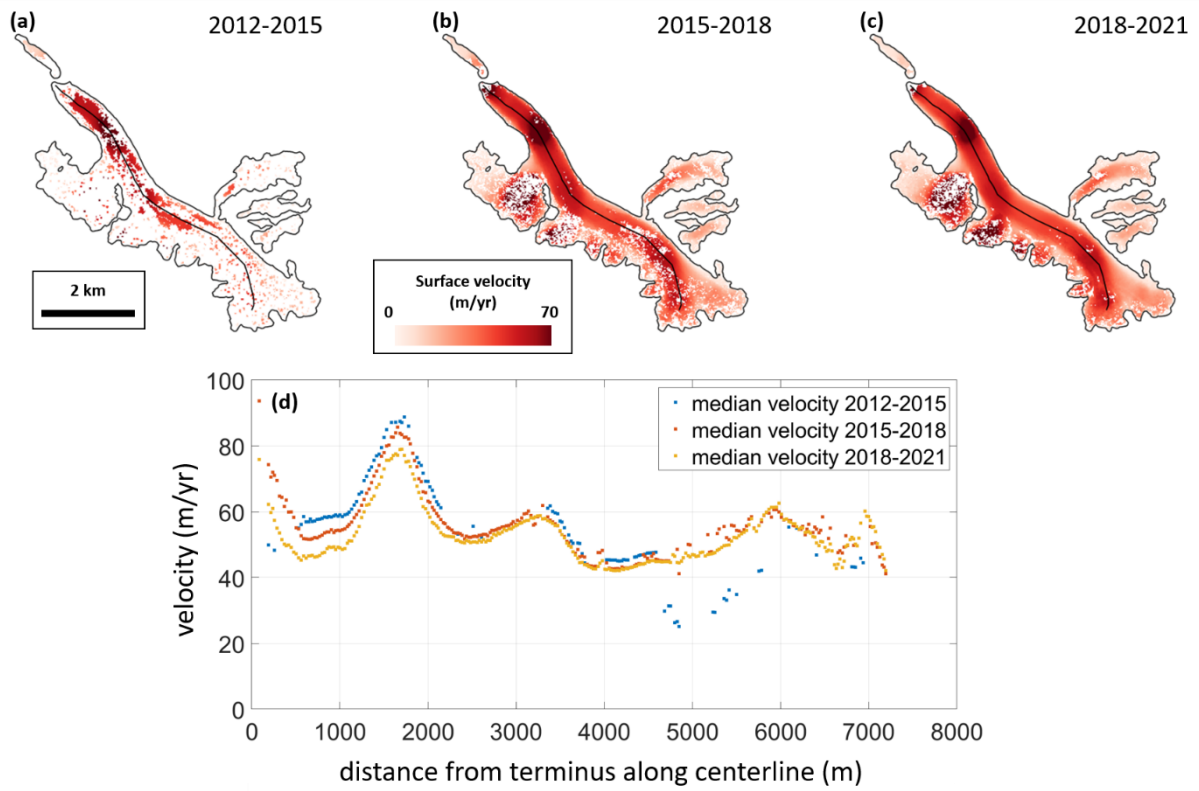


Figure S16: Median velocity over the (a) 2012-2015, (b) 2015-2018 and (c) 2018-2021 periods from all Pléiades orthoimage pairs, without any smoothing or gap filling. The black outlines indicate the glacier outlines manually derived from the 08/09/2020 Pléiades orthoimage and the black line shows the centerline along which velocity profiles were extracted (d).

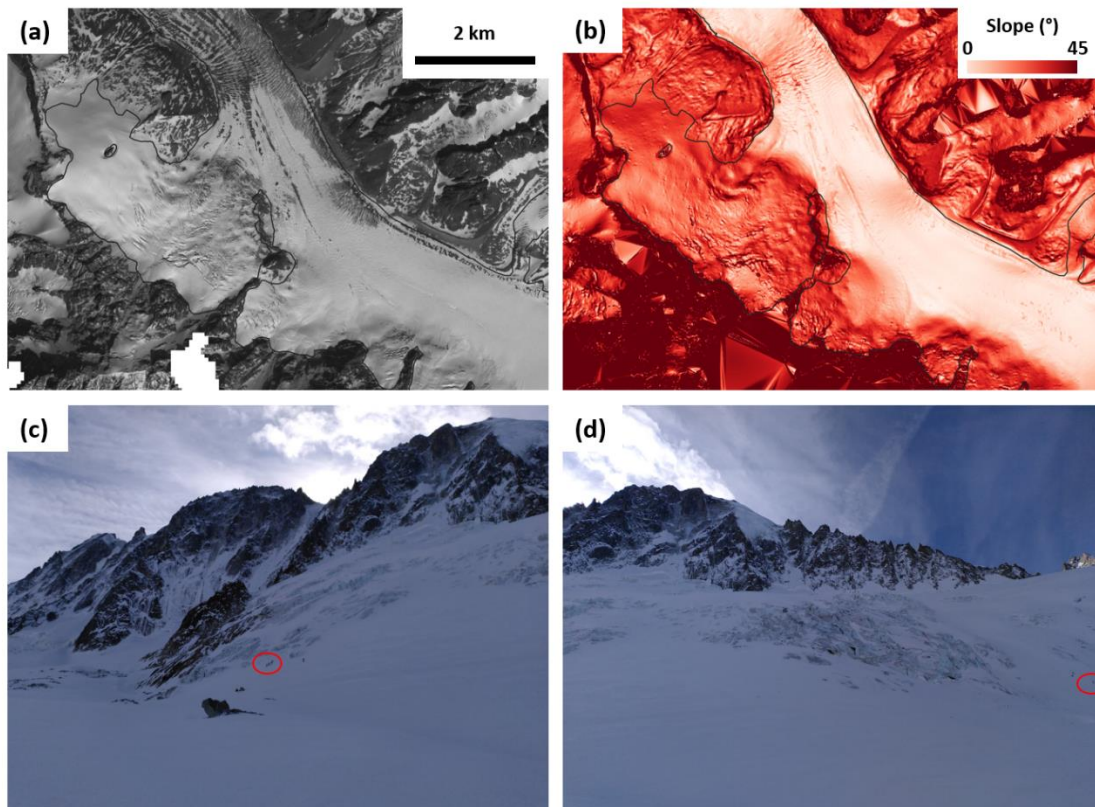


Figure S17: (a) Pléiades orthoimage of the Rognons tributary from 10/06/2017. (b) Slope of the 15/02/2017 reference mean DEM for the Rognons tributary and surroundings. The black glacier outlines were derived from a Pléiades orthoimage acquired on 08/09/2020. (c-d) Pictures of the Rognons tributary taken from the main glacier trunk on 06/02/2024. Skiers (circled in red) are visible in each image for scale.

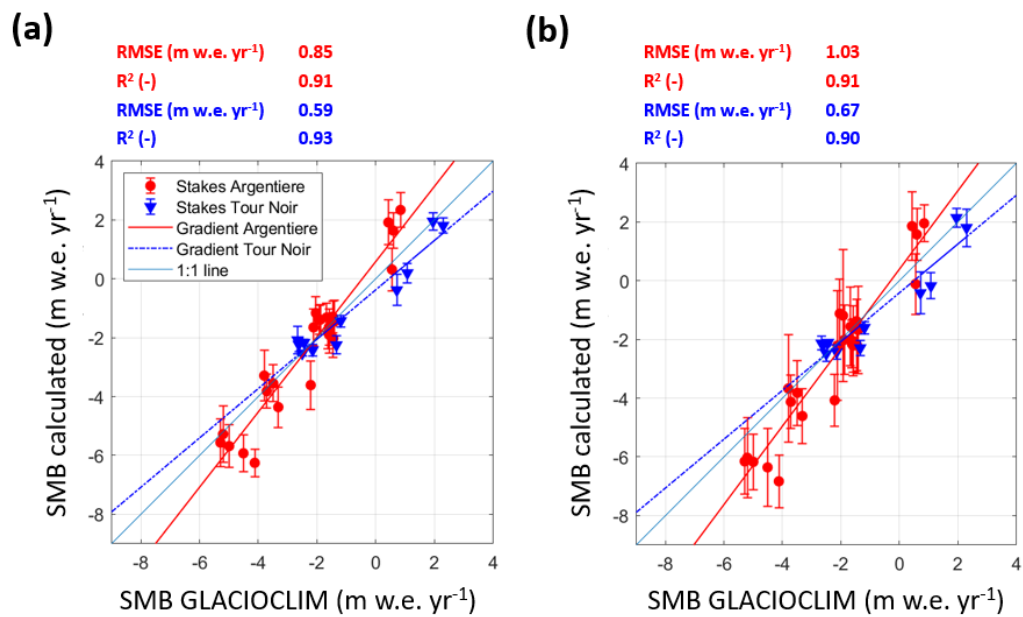


Figure S18: Direct comparison of mean annual SMB calculated with (a) the IGM modelling approach and (b) the IGM modelling approach after imposing the integral of the flux divergence to be zero in the inversion, with the mean annual mass balances over the period 2012-2021 from the stake measurements, at stake locations.

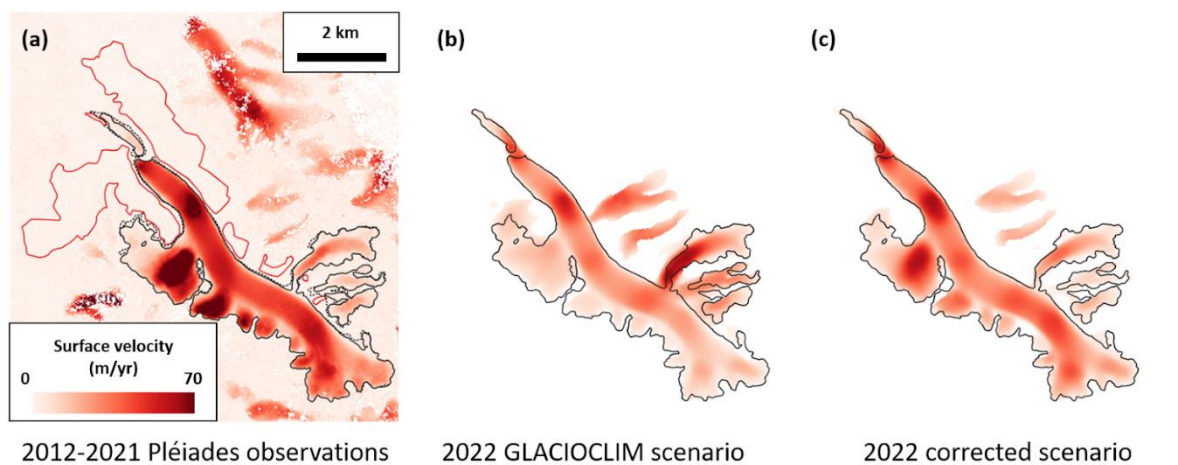


Figure S19: (a) Mean velocity over the 2012-2022 period from all 277 Pléiades orthoimage pairs. The red outlines show the zones of off-glacier stable terrain used to estimate the uncertainties of these products. The black outlines indicate the glacier outlines manually derived from the 08/09/2020 Pléiades orthoimage. (b) 2022 velocity from the GLACIOCLIM scenario. (c) 2022 velocity from the corrected scenario.